Shape of ^{80}Kr at high spin

G. Mukherjee,* H. C. Jain, R. Palit, P. K. Joshi, S. D. Paul, and S. Nagaraj
Department of Nuclear and Atomic Physics, Tata Institute of Fundamental Research, Mumbai, India
(Received 11 June 2000; revised manuscript received 4 May 2001; published 22 August 2001)

Lifetimes of eight high spin states were measured in the yrast band of even-even nucleus ^{80}Kr by Doppler shift attenuation method. High spin states were populated by the heavy ion fusion evaporation reaction ^{65}Cu(^{19}F,$2p2n$)^{80}Kr. The transition quadrupole moments, extracted from the lifetimes of the states, show a decreasing tendency after the band crossing indicating a change in shape of ^{80}Kr at high spin. The total Routhian surface calculations, using Woods-Saxon mean field potential and BCS pairing with Strutinsky shell correction procedure, predict a change from a near oblate to near prolate shape with small deformation along the yrast band at high spin in ^{80}Kr. The present experimental Q_t values and the second alignment in the yrast band of ^{80}Kr support the predicted change in shape.

DOI: 10.1103/PhysRevC.64.034316 PACS number(s): 21.10.Tg, 21.10.Ky, 21.60.Cs, 27.50.+e

I. INTRODUCTION

The ground states of krypton isotopes exhibit a wide variety of shapes as a function of neutron number. The measured lifetimes of the low-lying excited states indicate that the light krypton isotope ^{74}Kr is highly deformed ($\beta_2 \approx 0.37$) [1,2] while heavier isotope ^{82}Kr [3] is weakly deformed ($\beta_2 \approx 0.15$). Moreover, recent experimental as well as theoretical calculations indicate that the shape changes from near prolate in lighter krypton isotopes to near oblate in heavier isotope ^{80}Kr [1–8]. Due to this variation in ground state shapes, the high spin properties such as particle alignments and shape evolution of these nuclei as a function of spin also become very interesting.

Recent data on ^{76,78}Kr [4–7] provide some interesting observations at high spin. Both nuclei exhibit shape coexistence at low spins because of the competition between the proton and neutron deformed magic gaps in single particle energy diagram. The simultaneous alignments of proton and neutron pairs in ^{76}Kr could be explained [5] by assuming a prolate shape that changes over to a triaxial shape with positive γ due to the first proton alignment—thereby reducing the neutron alignment frequency. The change in shape was experimentally confirmed from the lifetime measurements of high spin states in this nucleus. In ^{78}Kr, the ambiguity of the nature of the first band crossing was removed by the g-factor measurement [9]. This measurement indicated that the first crossing in ^{78}Kr is due to a neutron pair alignment unlike in ^{76}Kr. The cranked shell model (CSM) calculations showed that both the band crossings observed in ^{78}Kr can be understood by assuming oblate deformation with $\beta_2 \approx 0.38$ [7]. The lifetime measurements showed that the deformation in ^{78}Kr reduces considerably after the second band crossing [7]. Thus, in view of these differences in high spin behavior of krypton isotopes, it becomes interesting to study high spin states in the neighboring isotope ^{80}Kr that is reported to have oblate ground state deformation [8].

The shape coexistence phenomenon is not observed in the ground state of ^{80}Kr unlike its lighter mass isotopes. This indicates that the shape driving competition of protons and neutrons does not occur for ^{80}Kr. This is because there is no large shell gap found for neutron number 44. The band structure of ^{80}Kr has been studied recently by Döring *et al.* [8]. The level scheme shows that the ground state positive parity band is crossed by a two-quasiproton (2qp) band at a rotational frequency $\hbar\omega \sim 0.5$ MeV and becomes yrast above the 8^+ state. The 2qp band has been extended up to 20^+ whereas the ground band was extended upto 16^+. The lifetime measurements of some of the states in yrast band were reported by Friederichs *et al.* [10] and Funke *et al.* [11] by recoil distance method (RDM) and Doppler shift attenuation methods (DSAM) methods. These studies indicate a quadrupole deformation with $\beta_2 \sim 0.25$ for low lying states of ^{80}Kr. Total Routhian surface (TRS) calculations [8] also suggest an oblate shape with similar β_2 in this nucleus. CSM calculations performed for an oblate shape with $\beta_2 \sim 0.25$ predict [8] the two-quasineutron alignment at $\hbar\omega \approx 0.50$ MeV and two-quasiproton alignment at $\hbar\omega \approx 0.72$ MeV. On the other hand, the observed gain in aligned angular momentum $\sim 6\hbar$ at $\hbar\omega \approx 0.5$ MeV indicates simultaneous alignment of two quasineutrons and two quasiprotons. Moreover, the lifetimes of the high spin states beyond the first band crossing are not known in ^{80}Kr. In order to understand, the particle alignment and shape of ^{80}Kr at high spins, the lifetimes of the high spin states in the yrast band of ^{80}Kr have been measured in the present work.

II. EXPERIMENTAL DETAILS AND DATA ANALYSIS

The lifetimes of the high spin states of ^{80}Kr were measured by DSAM. Levels of ^{80}Kr were populated by heavy ion fusion evaporation reaction ^{65}Cu(^{19}F,$2p2n$)^{80}Kr using 74-MeV ^{19}F beam from the 14UD Pelletron at Tata Institute of Fundamental Research, Mumbai. A thin natural Cu (31% ^{65}Cu) target with thickness ~ 850 μg/cm^2 and rolled onto an 8-mg/cm^2 thick Ta backing was used for the experiment. The thickness of backing was enough to stop the recoils. The maximum recoil velocity was $\sim 2.04\%$ of velocity of light.

*Present address: Department of Physics and Applied Physics, University of Massachusetts Lowell, One University Avenue, Lowell, MA 01854.

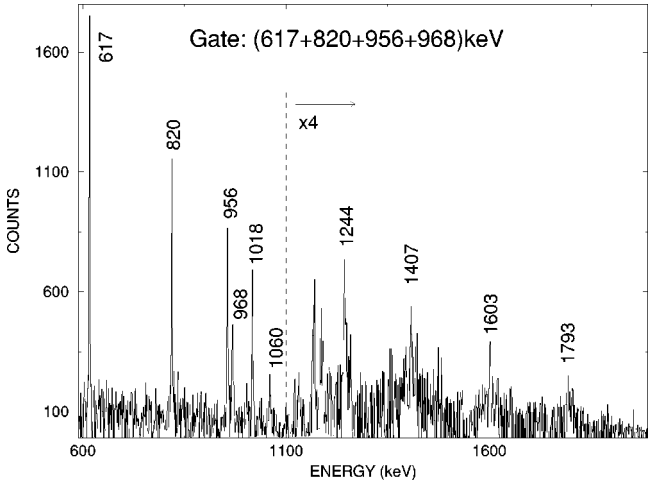

FIG. 1. Sum gated spectrum with data from all the detectors showing the γ-ray transitions of ^{80}Kr.

γ-γ coincidence data were taken in the list mode using three clovers and one HPGe detector with anti-Compton shields in all of them. The detectors were kept at 30°, 50°, 90°, and 110° angles with respect to the beam direction. A multiplicity filter consisting of 14-element NaI(Tl) detectors was also used in the experiment. The multiplicity condition $M \geqslant 2$ was set in the hardware electronics.

In the offline data analysis, data from all the detectors were gain matched to 0.5 keV/channel. A sum gated spectrum is shown in Fig. 1, which includes data from all the detectors. Data from detector at 50° were used for the DSAM analysis. For this, a $4K \times 4K$ γ-γ coincidence matrix was constructed with the spectrum from the 50° detector along one axis of the matrix and the spectra from rest of the detectors along the other axis.

All the transitions reported [8] for the yrast band of ^{80}Kr have been observed in the present experiment. Coincidence spectra gated by 617-keV, 820-keV, 956-keV, and 968-keV yrast transitions (see Fig. 2) were used for line-shape analysis. Gated spectra were compressed to 1.0 keV/channel for the analysis to improve counts/channel.

Analysis of the DSAM data were done with the help of the computer program LINESHAPE [12] (and references therein). The Monte Carlo simulation technique has been used in the program. It was initially applied by Baceler *et al.* [13,14] for the velocity and directional history of a series of recoiling nuclei. Shell corrected Northcliffe and Schilling [15] electronic stopping powers have been used in this program. The lifetime analysis program does a χ^2 minimization of the fit for (a) Q_t, the transition quadrupole moment for the transition of interest, (b) Q_t (SF), the transition quadrupole moment for the modeled side feeding (SF) transition, (c) a normalizing factor to normalize the intensity of the fitted transition, (d) the intercept and slope of a linear background, and (e) the intensities of contaminant peaks near the peak of interest. We have used rotational cascade side feeding model that consists of a five-state rotational band with fixed moment of inertia of $\sim 20\hbar^2$ MeV^{-1}. The effect of the variation of Q_t(SF) on the result of Q_t near the minimum was very small and remain within the error bar.

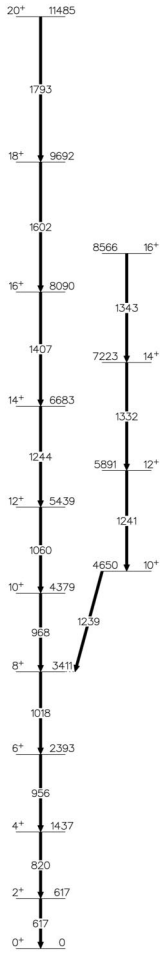

FIG. 2. Partial level scheme of ^{80}Kr.

The lifetimes of eight high-spin states upto the highest observed state at $20\hbar$ in the yrast band of ^{80}Kr were determined in the present work. The highest level was fitted first for effective lifetime without the side feeding correction and then the successive levels were fitted taking the top feeding and the side feeding into account. The experimental and fitted line shapes for the 956-, 1060-, 1244-, 1407-, 1603-, and 1793-keV γ rays are shown in Fig. 3. The final fits of the line shapes are represented by continuous curve, the dot-dashed curves are the line shape fit without taking into account the effect of contaminant peaks. The accompanied contaminant peaks near the peak of interests as simulated by the program are shown by the dashed curves.

III. RESULTS

The lifetimes (τ) measured in the present work and those reported by Funke *et al.* [11] are listed in Table I. The reduced transition strength $B(E2)$ and transition quadrupole moment Q_t were obtained from the lifetimes using the formulas

$$B(E2) = \frac{8.20 \times 10^{-10}}{E_\gamma^5 \ \tau} \quad e^2 \ \text{fm}^4, \tag{1}$$

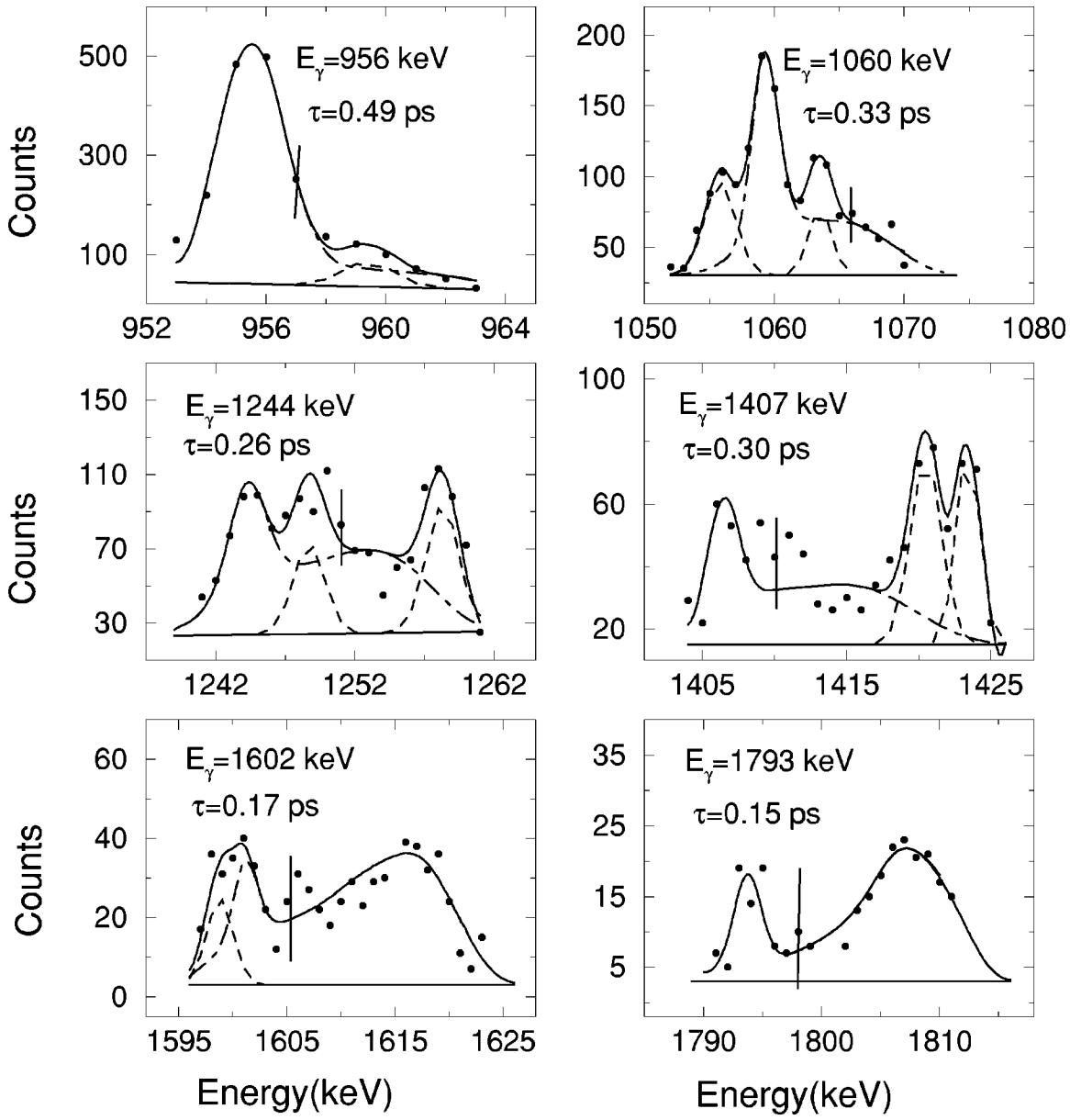

FIG. 3. The lineshape fits for six transitions in ^{80}Kr. The final fits of the lineshapes are shown by the continuous curve, the dashed-dot curve is the lineshape fit for the transition without taking into account the effect of contaminant peaks. The accompanied contaminant peaks near the peak of interests as simulated by the program along with the backgrounds are shown by the dashed lines.

where, τ is the lifetime (in sec) of the state and E_γ is the transition energy in MeV, and

$$B(E2,I\rightarrow I-2)=\frac{5}{16\pi}Q_t^2\langle I2K0|I-2K\rangle^2, \qquad (2)$$

where $B(E2)$ is in $e^2\mathrm{b}^2$ and quadrupole moment Q_t is in eb and the term in bracket is a Clebsch-Gordon coefficient. K is the projection of total angular momentum on the symmetry axis.

The lifetimes of the 2^+ and 4^+ levels, shown in the table, were measured earlier by RDM technique [11]. The earlier measurement by Funke *et al.* [11] were confined upto the 12^+ level. In the present work, the lifetime measurements have been extended upto the 20^+ state—the highest level observed in the yrast band. It can be seen from Table I that more precise values have been obtained for lower spin states in the present work.

The quadrupole moments Q_t in the yrast band are found to decrease by about 51% from an average value of $\sim$2.36 eb before the 12^+ state to a value of $\sim$1.15 eb at higher spins. This indicates a change in shape following the particle alignment at high spins for the yrast band of ^{80}Kr. Similar decrease in Q_t is observed for other krypton isotopes also [5,7]. This has been discussed in detail in the next section.

IV. DISCUSSION

The recent report on ^{80}Kr [8] suggests that a 2qp band crosses the positive parity ground band at a frequency $\hbar\omega$

TABLE I. Measured lifetimes (τ) in ps, transition strength [$BE(2)$] in Weisskopf unit (W.u.), transition quadrupole moments (Q_t) in eb, and the sidefeeding quadrupole moments (Q_{SF}) in eb for the yrast band in ^{80}Kr.

Transition $(I_i^\pi \rightarrow I_f^\pi)\hbar$	E_γ (keV)	τ (ps) Previous[a]	Present	$BE(2)$ (W.u.)[b]	Q_t (eb)	Q_{SF} eb
$2^+ \rightarrow 0^+$	617	12(1)		37(3)	1.95(8)	
$4^+ \rightarrow 2^+$	820	2.3(5)		47^{13}_{8}	$1.84^{.24}_{.17}$	2.10(24)
$6^+ \rightarrow 4^+$	956	1.0(4)	$0.49^{0.18}_{0.12}$	101^{32}_{27}	$2.57^{0.40}_{0.36}$	1.95(20)
$8^+ \rightarrow 6^+$	1018	$0.4^{0.4}_{0.2}$	$0.43^{0.09}_{0.07}$	84^{16}_{14}	$2.30^{0.22}_{0.20}$	3.51(45)
$10^+ \rightarrow 8^+$	968	$1.0^{0.6}_{0.4}$	$0.58^{0.12}_{0.10}$	81^{16}_{13}	$2.22^{0.21}_{0.20}$	1.86(26)
$12^+ \rightarrow 10^+$	1060	0.35(20)	$0.33^{0.05}_{0.06}$	91^{20}_{12}	$2.34^{0.22}_{0.17}$	2.50(32)
$14^+ \rightarrow 12^+$	1244	<1.0	$0.26^{0.08}_{0.07}$	50^{18}_{11}	$1.72^{0.29}_{0.20}$	2.97(28)
$16^+ \rightarrow 14^+$	1407		$0.30^{0.11}_{0.12}$	23^{15}_{6}	$1.18^{0.35}_{0.17}$	2.18(28)
$18^+ \rightarrow 16^+$	1602		$0.18^{0.07}_{0.07}$	21^{14}_{6}	$1.12^{0.30}_{0.19}$	1.65(26)
$20^+ \rightarrow 18^+$	1793		<0.15	>14	>0.90	

[a]Values taken from Funke *et al.* [11].
[b]1 W.u.$=20.5e^2$ fm^4.

≈ 0.50 MeV. This was initially interpreted as a proton alignments in Refs. [11,16] but later it was argued by Döring *et al.* [8] that the first crossing is due to the alignment of a pair of neutrons. The cranking calculations reproduce the crossing frequency for neutron at $\hbar\omega \approx 0.5$ MeV for an oblate shape with $\beta_2 \approx 0.25$. The lifetime measurements also indicate similar deformation for the yrast band before the first crossing. $J^{(2)}$ values of ^{80}Kr along the yrast band have been plotted in Fig. 4. This shows a second peak at $\hbar\omega \approx 0.52$ MeV after the first crossing at $\hbar\omega \approx 0.50$ MeV. In ^{76}Kr [4], the kink in the $J^{(2)}$ after the first crossing and the large gain in alignment were interpreted as almost simultaneous alignment of protons and neutrons. The experimental alignment (i_x) values are plotted in Fig. 5 for ^{76}Kr and ^{80}Kr. It can be seen that the gain in alignment for ^{80}Kr is about $6\hbar$ that is similar to that observed for ^{76}Kr. This indicates nearly simultaneous alignment of two quasineutrons and two quasiprotons in ^{80}Kr also. However, the simultaneous alignment could not be explained as proton pair alignment followed by neutron pairs in the CSM calculations in Ref. [8] where an oblate shape was assumed to persist beyond the first band crossing. Infact it gives a much larger value ≈ 0.72 MeV for the two-quasiproton band crossing.

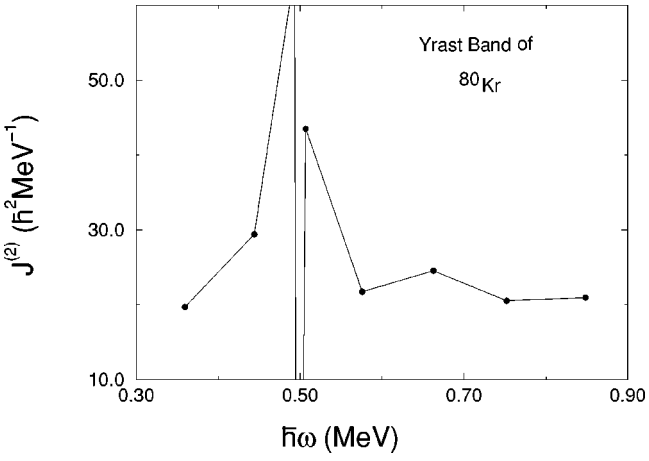

FIG. 4. Dynamic moments of inertia $J^{(2)}$ plotted as a function of rotational frequency $\hbar\omega$ for the positive parity yrast band of ^{80}Kr.

In ^{76}Kr, the early second crossing and thus the simultaneous alignment was explained as arising due to a change in shape after the first proton alignment [4]. Later the lifetime measurements [5] confirmed the shape change towards positive γ in accordance with the cranked shell model calculations. In ^{74}Kr also, the lifetime measurements show a clear shape change induced by particle alignment [17]. The lifetime measurements of the high spin states in the present work indicate a decrease in the quadrupole moment Q_t (see Fig. 6) after the first crossing in the yrast band of ^{80}Kr. This indicates a less deformed shape after the first neutron alignment. The CSM calculations show that the proton alignment frequency for ^{80}Kr comes down to a value $\hbar\omega = 0.52$ MeV in agreement with the experimental value for a less deformed prolate shape as discussed in the next section.

V. CRANKED SHELL MODEL CALCULATIONS

The Hartree-Fock-Bogoliubov cranking model calculations with Woods-Saxon potential and monopole pairing [18,19] have been performed in the present work to have a better understanding of the shape and particle alignments in the yrast band of ^{80}Kr at high spin. In these calculations, the pairing term was calculated by solving the BCS gap equation at rotational frequency $\omega = 0$ using the interaction strength G obtained from the systematics. The pairing gap Δ was allowed to vary smoothly as a function of ω for higher frequencies in such a way that the value of Δ drops to $\Delta_\bigcirc/2$ (where $\Delta_\bigcirc$ is the gap parameter at $\omega = 0$) at a frequency ω_c. The values of ω_c for protons and neutrons were taken as $\omega_c^\pi = 1.15$ MeV and $\omega_c^\nu = 0.95$ MeV, respectively. The TRS were calculated in a β_2-γ mesh for the yrast band of ^{80}Kr within this model including the Strutinsky shell correction. These were calculated at various values of rotational frequency $\hbar\omega$ and at each value of (β_2, γ) the total energy was

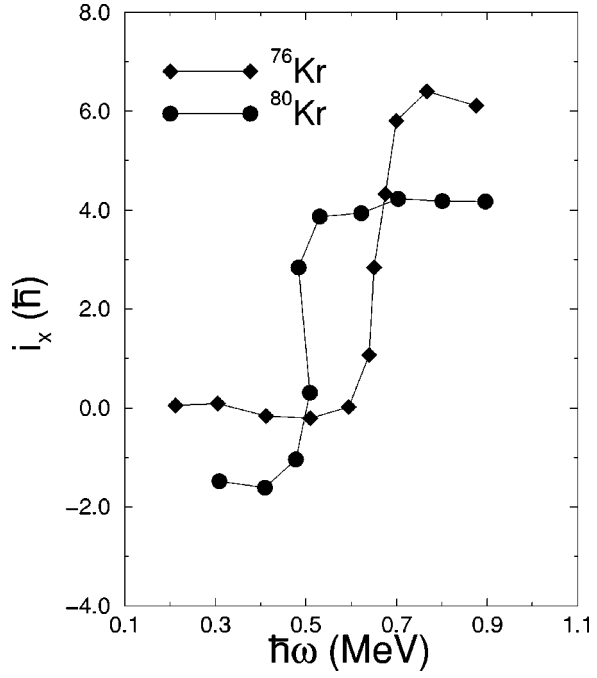

FIG. 5. Aligned angular momentum i_x plotted as a function of rotational frequency $\hbar\omega$ for the positive parity yrast band of ^{76}Kr and ^{80}Kr. The Harris parameters $I_{\bigcirc}=3.5\hbar$ and $I_1=21\hbar$ MeV^{-1} were used for reference configuration.

minimized with respect to the hexadecouple deformation β_4.

The total Routhian surfaces for the yrast band of ^{80}Kr are shown in Fig. 7 and calculated for two values of rotational frequencies—one at $\hbar\omega=0.30$ MeV corresponds to the situation before the band crossing and the other at $\hbar\omega=0.60$ MeV corresponding to the situation after the band crossing. It can be seen that the TRS at $\hbar\omega=0.30$ MeV indicates an oblate shape with $\beta_2\approx 0.26$, $\gamma\approx -55°$, and β_4

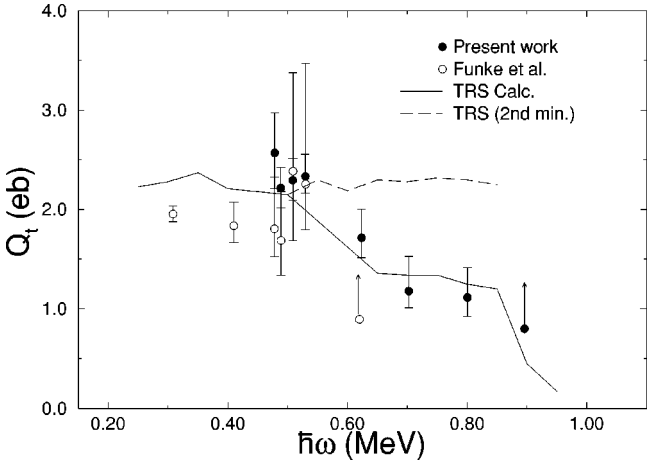

FIG. 6. The quadrupole moment Q_t for the positive parity yrast band of ^{80}Kr as a function of rotational frequency $\hbar\omega$. The filled circles correspond to the experimental data from the present work while the open circles correspond to the data from Ref. [11]. The theoretical values are shown by the solid curve corresponding to the minimum value of the TRS and the dashed curve corresponds to the second minimum in the TRS after the first band crossing.

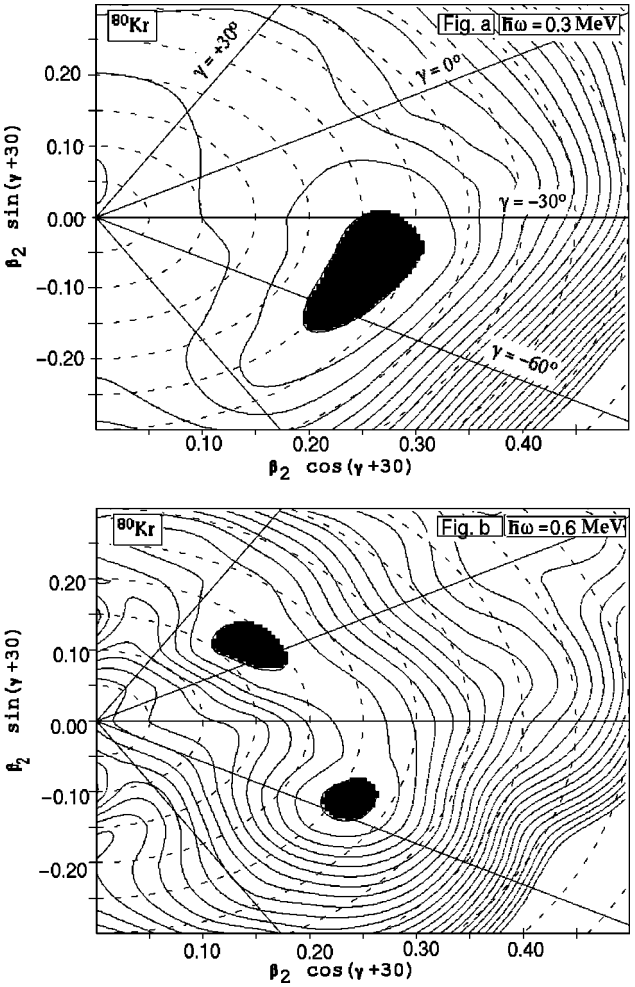

FIG. 7. Total Routhian surface plots in the β_2-γ plane for the yrast band of ^{80}Kr. These are shown for two rotational frequencies $\hbar\omega=0.30$ MeV and 0.60 MeV corresponding to frequencies before and after the band crossing, respectively. The energy separation between the contours is 250 keV.

≈ -0.016 that is similar to the one reported in Ref. [8]. The situation after the band crossing changes quite drastically as can be seen from the TRS at $\hbar\omega=0.60$ MeV. Two minima appear in this case that are within 250 keV in energy. The first one has a near prolate shape with small deformation $\beta_2\approx 0.18, \gamma\approx +4.6°$, and $\beta_4\approx -0.01$ while the other one has a near oblate shape similar to that before the band crossing.

The theoretical values of quadrupole moments were obtained by calculating the Q_{th} from the (β_2,γ) values corresponding to the minimum energy of the TRS using the formula [20]

$$Q_{th}=\frac{6Zr^2}{15\pi}\beta_2(1+0.36\beta)\cos(\gamma+30°). \tag{3}$$

The quadrupole moment Q_{th} thus obtained for various values of rotational frequency $\hbar\omega$ are compared with the experimental values in Fig. 6. The filled circles in Fig. 6 correspond to the Q_t as obtained in the present experiment while the open circles correspond to the experimental values from

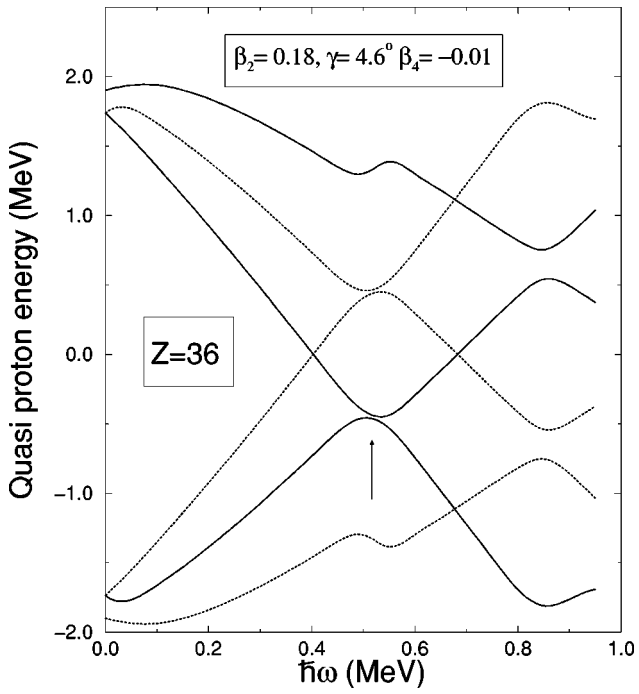

FIG. 8. Calculated single particle Routhians for protons in ^{80}Kr as a function of rotational frequency $\hbar\omega$. The calculations are performed for deformation $\beta_2=0.18$, $\gamma=4.6°$, and $\beta_4=-0.01$. The crossing point is shown by the arrow.

Ref. [11]. The solid line corresponds to the theoretical values Q_{th} for the lower minimum in the TRS while the dashed line corresponds to the Q_{th} calculated for the second minimum in the TRS.

It can be seen from Fig. 6 that the experimental quadrupole moments match quite well with the theoretical values before the band crossing. Q_{th} values calculated for the first (prolate) minimum after the first band crossing also match quite well with the experimental values. This indicates a change in shape from near oblate to near prolate along the yrast band of ^{80}Kr at high spin. The level scheme of ^{80}Kr [8] shows that the ground band (g band in Fig. 2) continues through the nonyrast levels after the band crossing upto 16^+. This band might correspond to the second minimum in the TRS. However, lifetime of levels in this band could not be obtained from the present work. It would be very interesting to measure the lifetimes in this band and compare with the calculated values of quadrupole moments.

The single particle Routhians for protons in ^{80}Kr were calculated for a near prolate shape with $\beta_2=0.18, \gamma=4.6°$, and $\beta_4=-0.01$ corresponding to the shape of the yrast band at higher rotational frequency and are plotted in Fig. 8. This figure shows a band crossing (identified by an arrow), corresponding to two-quasiproton alignment at a frequency $\hbar\omega \approx 0.52$ MeV, a value close to the quasineutron alignment frequency and thus provides extra support to the proposed simultaneous alignment.

VI. CONCLUSIONS

Lifetimes of the high spin states have been measured upto the highest observed state at $20\hbar$ in the yrast band of ^{80}Kr. The transition quadrupole moments extracted from the lifetimes indicate a change in shape at high spin for this band. TRS calculations suggest that the change in quadrupole moment is due to change in shape in ^{80}Kr from near oblate to near prolate with lower deformation at high spin. The large gain in aligned angular momentum demanded almost simultaneous alignment of neutron and proton pairs. The dynamic moments of inertia $J^{(2)}$ also suggested a second band crossing very near to the first one for the yrast band of ^{80}Kr. The cranking calculations show that the change from oblate to near prolate shape with lower deformation brings down the frequency of the two-quasiproton band crossing to a value close to the two quasineutron band crossing frequency with prolate shape.

ACKNOWLEDGMENTS

We gratefully acknowledge the help of all the pelletron staff for smooth functioning of the accelerator. The help of A. Mahadkar in preparing the target is acknowledged. We would also like to thank S. Chanda for his help and participation during the experiments.

[1] S.L. Tabor, P.D. Cottle, J.W. Holcomb, T.D. Johnson, P.C. Womble, S.G. Buccino, and F.E. Durham, Phys. Rev. C **41**, 2658 (1990).

[2] J. Heese, D.J. Blumenthal, A.A. Chishti, P. Chowdhury, B. Crowell, P.J. Ennis, C.J. Lister, and Ch. Winter, Phys. Rev. C **43**, R921 (1991).

[3] P. Kemnitz, P. Ojeda, J. Doring, L. Funke, L.K. Kostov, H. Rotter, E. Will, and G. Winter, Nucl. Phys. **A425**, 493 (1984).

[4] C.J. Gross, J. Heese, K.P. Lieb, S. Ulbig, W. Nazarewicz, C.J. Lister, B.J. Varley, J. Billowes, A.A. Chishti, J.H. McNeill, and W. Gelletlyi, Nucl. Phys. **A501**, 367 (1989).

[5] G. Mukherjee, Ph.D. thesis, Visva Bharati University, Santiniketan, India, 1999.

[6] H. Sun, J. Doring, G.D. Johns, R.A. Kaye, G.Z. Solomon, S.L. Tabor, M. Devlin, D.R. LaFosse, F. Lerma, D.G. Sarantites, C. Baktash, D. Rudolph, C.-H. Yu, I.Y. Lee, A.O. Macchiavelli, I. Birriel, J.X. Saladin, D.F. Winchell, V.Q. Wood, and I. Ragnarsson, Phys. Rev. C **59**, 655 (1999).

[7] P. K. Joshi *et al.* (private communication).

[8] J. Doring, V.A. Wood, J.W. Holcomb, G.D. Johns, T.D. Johnson, M.A. Riley, G.N. Sylvan, P.C. Womble, and S.L. Tabor, Phys. Rev. C **52**, 76 (1995).

[9] J. Billowes, F. Cristancho, H. Grawe, C.J. Gross, J. Heese, A.W. Mountford, and M. Weiszflog, Phys. Rev. C **47**, R917 (1993).

[10] H.-G. Friederichs, A. Gelberg, B. Heits, K.P. Lieb, M. Uhrmacher, K.O. Zell, and P. von Brentano, Phys. Rev. Lett. **34**, 745 (1975).

[11] L. Funke, J. Doring, F. Dubbers, P. Kemnitz, E. Will, G. Winter, V.G. Kiptilij, M.F. Kudojarov, I.Kh. Lemberg, A.A. Paster-

nak, A.S. Mishin, L. Hildingsson, A. Johnson, and Th. Lindblad, Nucl. Phys. **A355**, 228 (1981).
[12] N.R. Johnson, J.C. Wells, Y. Akovali, C. Baktash, R. Bengtsson, M.J. Brinkman, D.M. Cullen, C.J. Gross, H.-Q. Jin, I.-Y. Lee, A.O. Macchiavelli, F.K. McGowan, W.T. Milner, and C.-H. Yu, Phys. Rev. C **55**, 652 (1997).
[13] J.C. Bacelar, A. Holm, R.M. Diamond, E.M. Beck, M.A. Deleplanque, J. Draper, B. Herskind, and F.S. Stephens, Phys. Rev. Lett. **57**, 3019 (1986).
[14] J.C. Bacelar, R.M. Diamond, E.M. Beck, M.A. Deleplanque, J. Draper, and F.S. Stephens, Phys. Rev. C **35**, 1170 (1987).
[15] L.C. Northcliffe and R.F. Schilling, Nucl. Data Tables **7**, 233 (1970).
[16] D.L. Sastry, A. Ahmed, A.V. Ramayya, R.B. Piercey, H. Kawakami, R. Soundranayagam, J.H. Hamilton, C.F. Maguire, A.P. de Lima, S. Ramavataram, R.L. Robinson, H.J. Kim, and J.C. Wells, Phys. Rev. C **23**, 2086 (1981).
[17] A. Algora, G. de Angelis, F. Brandolini, R. Wyss, A. Gadea, E. Farnea, W. Gelletly, S. Lunardi, D. Bazzacco, C. Fahlander, A. Aprahamian, F. Becker, P.G. Bizzeti, A. Bizzeti-Sona, D. de Acuna, M. De Poli, J. Eberth, D. Foltescu, S.M. Lenzi, T. Martinez, D.R. Napoli, P. Pavan, C.M. Petrache, C. Rossi Alvarez, D. Rudolph, B. Rubio, S. Skoda, P. Spolaore, R. Menegazzo, H.G. Thomas, and C.A. Ur, Phys. Rev. C **61**, 031303(R) (2000).
[18] W. Nazarewicz, J. Dudek, R. Bengtsson, T. Bengtsson, and I. Ragnarsson, Nucl. Phys. **A435**, 397 (1985).
[19] W. Nazarewicz, M.A. Riley, and J.D. Garrett, Nucl. Phys. **A512**, 61 (1990).
[20] J.C. Lisle, R. Chapman, F. Khazaie, J.N. Mo, H. Hübel, W. Schmitz, K. Theine, J.D. Garrett, G.B. Hagemann, B. Herskind, and K. Schiffer, Nucl. Phys. **A520**, 451c (1990).